Polymer-in-a-Silica-Crust Membranes: Macroporous Materials with Tunable Surface Functionality

Ana M. Urmenyi,[†,§] Albert P. Philipse,[‡] Rob G. H. Lammertink,[†] and Matthias Wessling*[,†]

Membrane Technology Group, Faculty of Science and Technology, University of Twente, P.O. Box 217, 7500 AE, Enschede, The Netherlands, and Van't Hoff Laboratory for Physical and Colloid Chemistry, Debye Institute, Utrecht University, Padulaan 8, 3584 CH, Utrecht, The Netherlands

Received January 14, 2006. In Final Form: March 30, 2006

We report on alkaline hydrolysis of tetraethoxysilane (Stöber synthesis) inside a macroporous polymer matrix resulting in a homogeneous coverage of silica onto the polymer surface. The encapsulation of the polymer struts by a continuous silica crust allows further functionalization with hydrophilic and hydrophobic silylating agents. The porous silica polymeric hybrid material combines the morphological control and mechanical flexibility of the polymeric matrix with the convenient surface modifications developed for glass and amorphous silica. This concept is applied to macroporous membranes where alteration in surface functionality allows tuning of hydrophobicity (contact angle and liquid entry pressure), streaming potential, and adsorption capacity of double-stranded DNA.

1. Introduction

Various surface treatments and modifications of macroporous polymers have been reported.[1] Surface modification of such materials may involve quite a number of chemical steps.[2] An important limiting factor is the availability of reactive groups such as (−OH, $-NH_2$, −SH, −COOH) that can undergo further chemical modifications.[3,4] Macroporous materials that lack reactive groups are occasionally pretreated by harsh methods employing, for example, oxidation reactions and plasma treatment.[5]

Inorganic surfaces, in contrast, can be modified easily with a large variety of functional moieties via condensation reactions at room (or slightly elevated) temperature. In particular, the covalent binding of silane coupling agents (SCAs) to amorphous silica or glass surfaces is well documented.[6,7] SCAs are being used to functionalize colloidal silica,[8,9] as well as larger silica spheres for chromatography. Much attention has also been given to graft surface groups on desire surfaces[1] for the subsequent covalent binding of biomolecules such as antibodies,[10] enzymes,[11] or supramolecular compounds.[12] In addition, (silylated) silica has appeared to be very suitable for DNA adsorption[13] with a purification purpose to remove DNA fragments from complex protein mixtures.

Though inorganic silica-based macroporous materials may have an advantage in comparison to polymer materials when it comes to surface modification, there are also drawbacks: inorganic macroporous materials are often based on sintering of spherical particles, which limits the resulting pore structure to packed-bed-like morphologies. Further sintering results only in densification of the existing morphology and reduced porosity. Morphologies with porosity gradients are difficult to synthesize.

There exist many methods to prepare macroporous polymers. Generally, these methods rely on the phase separation of polymer solutions. Disturbance of the thermodynamic equilibrium due to changes in temperature and solution composition results in thermally or diffusion induced phase separation (TIPS and DIPS, respectively). The resulting morphologies are complex but can be controlled extremely well. Porosities can vary significantly; pore sizes can be adjusted from micrometers down to nanometers. Such structures are normally opaque due to light scattering at the polymer−pore interface. Application of these morphologies is realized on a very large scale in the production of synthetic membranes. We propose to combine the versatility of silica-based functionalization with morphological and mechanical benefits of macroporous polymers by depositing an amorphous silica layer on a macroporous polymer matrix.

A few studies have explored the precipitation of silica on a polymer template via acid hydrolysis of silicon alkoxides.[14−17] At low pH, silica generally forms gel-like layers, rather than separate, discrete particles. It was our intention to also introduce silica in the form of discrete colloidal particles, which may either form ordered layers of well-defined spheres on the polymer surface or more disordered deposits of finely divided entities with high surface area. For the synthesis of the discrete silica particles, we use the well-known Stöber procedure, comprising

* To whom correspondence should be addressed. Phone: x-31 53 489 2950. Fax: x-31 53 489 4611. E-mail: m.wessling@utwente.nl.

† University of Twente.

‡ Utrecht University.

§ Present address: Nalco, Water R&D Europe, Ir. G.Tjalmaweg 1, 2342 BV, Oegstgeest, The Netherlands.

(1) Klein, E. *J. Membr. Sci.* **2000**, *179* (*1*−*2*), 1−27.

(2) Hennion, M.-C.; Pichon, V. *J. Chromatogr. A*, **2003**, *1000*, 29−52.

(3) Zou, H.; Luo, Q.; Zhou, D. *J. Biochem. Biophys. Methods* **2001**, *49*, 199−240.

(4) Urmenyi, A. M.; Poot, A. A.; Wessling, M.; Mulder, M. H. V. *J. Membr. Sci.* **2005**, *259* (*1*−*2*), 91−102.

(5) Mukherjee, D.; Kulkarni, A.; Gill, W. N. *J. Membr. Sci.* **1994**, *97*, 231−249.

(6) Plueddeman, E. *Silane coupling Agents*; Plenum: New York/London, 1982.

(7) Jal, P. K.; Patel, S.; Mishra, B. K. *Talanta* **2004**, *62*,1005−1028.

(8) Philipse, A. P.; Vrij, A. *J. Colloid Interface Sci.* **1989**, *128*, 121−136.

(9) Pathmamanoharan, C. *Colloids Surf.* **1990**, *50*, 1−6.

(10) Huang, S. C.; Caldwell, K. D.; Lin, J.-N.; Wang, H.-K.; Herron, J. N. *Langmuir* **1996**, *12*, 4292−4298.

(11) Pijanowska, D. G.; Remiszewska, E.; Lysko, J. M.; Jazwinski, J.; Torbicz, W. *Sens. Actuators, B* **2003**, *91*, 152−157.

(12) Nechifor, A. M.; Philipse, A. P.; de Jong, F.; van Duynhoven, J. P. M.; Egberink, R. J. M.; Reinhoudt, D. N. *Langmuir* **1996**, *12* (16), 3844−3854.

(13) Melzak, K. A.; Sherwood, C. S.; Turner, R. F. B.; Haynes, C. A. *J. Colloid Interface Sci.* **1996**, *181*, 635−644.

(14) Antonietti, M. Berton, B.; Göltner, C.; Hentze, H.-P. *Adv. Mater*. **1998**, *10* (2), 154−159.

(15) Colombo, P.; Bernardo, E. *Compos. Sci. Technol.* **2003**, *63* (16), 2353−2359.

(16) Zhang, H.; Hardy, G. C.; Rosseinsky, M. J.; Cooper, A. I. *Adv. Mater*. **2003**, *15* (1), 78−81.

(17) Zhang, H.; Hardy, G. C.; Khimyak, Y. Z.; Rosseinsky, M. J.; Cooper, A. I. *Chem. Mater*. **2004**, *16*, 4245.

10.1021/la060137o CCC: $33.50
Published on Web 05/10/2006

alkaline hydrolysis of tetraethoxysilane (TEOS) in an aqueous ethanol solution,[18] which to our knowledge has not been applied earlier in combination with macroporous polymers.

With respect to the use of such macroporous silica−polymeric materials in separation techniques, the literature on functionalized 'pure' silica suggests many possibilities. Examples are the separation of various precious metals such as Ru,[19] Pb,[20] and Cr,[21] preconcentration of heavy-metal ions from water solutions,[22,23] and the removal of DNA for purification purposes.[24] In the latter case, two different surfaces were studied, namely, bare silica and silica modified with 3-aminopropyltriethoxysilane (APS).[25]

This paper reports the preparation and properties of three different macroporous polymeric precursor materials that are subsequently encapsulated in a silica layer. This layer is further functionalized by silylation. The functionalized macroporous silica−polymer hybrid materials are either hydrophobic due to modifications with octadecyl silane or fluorinated silane coupling agent or hydrophilic due to grafting of aminated silane coupling agent on the silica surface. Furthermore, we study the feasibility of silica−hybrid membrane and aminated silica−hybrid membrane for DNA adsorption.

The various surface modifications of the starting polymeric material (silica deposition and further reactions with SCAs) are monitored with various techniques such as confocal microscopy and X-ray photoelectron spectroscopy (XPS). Water permeation properties are characterized to study liquid entry pressure effects: streaming potentials are measured as a sensitive indication for the various adjustments of the electrokinetic surface properties.

2. Experimental Section

2.1. Materials and Methods. All chemicals were used as supplied unless stated otherwise. Copolymer ethylene vinyl alcohol with an average of 27 mol% ethylene (EVAL 27) (Aldrich) and 44% (EVAL44), respectively (Aldrich), and polyethersulfone (PES) (BASF) were used for membrane preparation without further modification. Dimethyl sulfoxide (DMSO) and *N*-methylpyrolidone (NMP) were used as solvents. 1-Octanol (Aldrich) was used as an additive in the EVAL 27 and EVAL 44 membranes, while poly(vinyl pyrolidone) K 90 (PVP, Fluka) was used as an additive for PES membranes. All membranes were prepared by immersion precipitation.

2.2. EVAL 44 Membrane Preparation. 14% (w/w) polymer was dissolved in DMSO containing 14% (w/w) 1-octanol at 50 °C. After deaeration, the polymeric solution was cast onto a glass plate with a casting knife at room temperature and then immersed in a water bath at 40−45 °C. The membranes were subsequently washed with water and dried.[26]

2.3. EVAL 27 Membrane Preparation. 14% polymer EVAL 27 was dissolved at 50 °C in DMSO to which 25% 1-octanol was added as additive. After deaeration, the polymeric solution (40−45 °C) was cast onto a glass plate at 45 °C with a casting knife and then immersed in a water bath at 70−75 °C. The membranes were subsequently washed with water and dried at room temperature.

2.4. PES Membrane Preparation. 15% PES polymer and 10% PVP were dissolved in NMP. After deaeration, the polymeric solution was cast onto a glass plate with a casting knife at room temperature, immersed in a 65/35 NMP/water coagulation bath for 30 s, immersed in a water bath at 35−40°C, thoroughly washed with water, and dried at room temperature.

2.5. Stöber Silica Deposition (EVAL 27-T, EVAL 44-T, and PES-T). The EVAL 27, EVAL 44, and PES membranes were immersed for 24 h in 3.5% aqueous ammonia. The wet membranes were blotted carefully with filter immersed in tetraethylethoxy silane (Aldrich, TEOS) ethanol solution (1:15 v/v). After 2 h, a solution of ammonia in ethanol (1:1 v/v ammonia/TEOS) was added to the mixture. A correction of ammonia concentration has to be done depending on each membrane's swelling degree. The membranes were removed after 90 min from the mixture and dried for 24 h between two glass plates in air without removing the liquid trapped inside the pores. Afterward, the membranes were washed thoroughly with ethanol and water and dried at room temperature between two glasses plates. Blank membranes for water flux measurements were prepared by subjecting them to the same procedure, in the absence of TEOS.

2.6. Further Silica Growth (EVAL 27-T-G, EVAL 44-T-G, and PES-T-G). Ten circular (2.5 cm diameter) silica-coated membranes were added to a mixture of ammonia ethanol solution (1:35 v/v) and agitated for 1 h at room temperature (25 °C). Then, TEOS (1:1000 v/v) was added followed by continuous shaking for 24 h at room temperature. This procedure was repeated four times without any visible silica particle formation. The membranes were washed thoroughly with ethanol and distilled water and dried at room temperature between two glass plates.

2.7. Membrane Surface Modification. 2.7.1. 1*H*,1*H*,2*H*,2*H*-Perfluorooctyltrichlorosilane (FOTS). PES -T, EVAL 27-T, and EVAL 44-T were reacted with FOTS for 1.5 h at 120 °C in a closed vessel. After reaction the membranes were washed with ethanol and water and then dried at room temperature, the presence of FOTS was determined by XPS and indirectly by measurements of contact angle and liquid entry pressure.

2.7.2. Octadecyltricholorosilane (OTS) (Cl_3SiC_{18}). EVAL 27-T and EVAL 44-T were reacted in dry tetrahydrofuran (THF) with Cl_3SiC_{18} under reflux and argon atmosphere. After 24 h, the membranes (now coded EVAL 27-T-OTS and EVAL44-T-OTS) were washed with THF and ethanol and dried.

2.7.3. 3-Aminopropyltrimethoxysilane (APS). EVAL 27-T and EVAL 44-T were reacted in dry THF with APS under reflux and argon atmosphere. After 24 h, the membranes EVAL 27-T-NH_2 and EVAL44-T-NH_2 were carefully washed with THF, ethanol, and distilled water and dried. The presence of NH_2 groups was determined qualitatively by attenuated total reflectance Fourier transform infrared spectroscopy (ATR-FTIR), XPS, contact angles, confocal microscopy, and streaming potentials and quantitatively using the *N*-succinimidyl-3-(2-pyridyldithio) propionate (SPDP, Pierce) reaction as described elsewhere.[27]

2.7.4. 3-Aminopropyltrimethoxysilane (APS), Alternative Method. Three circular membranes were equilibrated for 30 min in 60 mL of ethanol to which 1 mL of NH_4OH (25% water solution) was added. Separately in a 100 mL closed vial, 60 mL of ethanol and 0.5 mL of APS were mixed. The membranes were added to the mixture and stirred gently for 24 h at 50 °C. No particle formation was visible. The membranes were thoroughly washed with ethanol and then dried at room temperature.

2.8. Quantitative Determination of Amino Groups. Seventy five milligrams of dried circular membranes (EVAL 27T-NH_2, EVAL44-T-NH_2, and PES-T-NH_2, respectively) 2.5 cm in diameter, were soaked in 1.5 mL of dry ethanol prepared according to standard purification methods[28] and reacted at room temperature with 0.5 mL

(18) Stöber, W.; Fink, A.; Bohn, E. *J. Colloid Interface Sci.* **1968**, *26*, 62−69.
(19) Vlašánkova, R.; Otruba, V.; Bendl, J.; Fišera, M.; Kanický, V. *Talanta* **1999**, *48*, 839−846.
(20) Ekinci, C.; Köklü, Ü. *Spectrochim. Acta, Part B* **2000**, *55* (9), 1491−1495.
(21) Hajkova, J.; Kanicky, V.; Otruba, V. *Collect. Czech. Chem. Commun.* **2000**, *65*. 1848−1864.
(22) Takman, N.; Akman, S.; Ozcan, M.; Köklu, U. *Anal. Bioanal. Chem.* **2002**, *374* (5), 977−980.
(23) Espinola, J. G. P.; Oliverira, S. F.; Lemus, W. E. S.; Souza, A. G.; Airoldi, C.; Moreira, J. C. A. *Colloids Surf., A* **2000**, *166*, 45−50.
(24) Tian, H.; Hühmer, A. F. R.; Landers, J. P. *Anal. Biochem.* **2000**, *283* (2), 175−191.
(25) Carré, A.; Lacarrière, V.; Birch, W. *J. Colloid Interface Sci.* **2003**, *260*, 49−55.
(26) Avramescu, M. E.; Sager, W. F. C.; Mulder, M. H. V.; Wessling, M. *J. Membr. Sci.* **2002**, *210*, 155−173.
(27) Ngo, T. T. *J. Biochem. Biophys. Methods* **1986**, *12* (5−6), 349−354.
(28) Perrin, D. D.; Armarego, W. L. F. *Purification of Laboratory Chemicals*; Pergamon Press: Elmsford, NY, 1989; p 174.

3-(2-pyridyldithio)propionic acid *N*-hydroxysuccinimide ester (SPDP) ethanol solution (12 mg/mL) and 3 mg of 4-methylaminopyridine as catalyst. After 30 min, the membranes were removed from the reaction mixture and subsequently washed with ethanol, demi-water, 1 M NaCl, and 1 M $NaHCO_3$, and finally soaked in 4 mL 0.1 M $NaHCO_3$ for 30 min. Next, the membranes were immersed in 4 mL of 50 mM 1,4-dimercapto-2,3-butanediol (DTT) in distilled water for about 15 min at room temperature to release pyridine-2-thione. The liquid was then diluted four times with 0.1 M $NaHCO_3$ followed by absorbance measurements at 343 nm against diluted 50 mM DTT as blank. The molar absorption coefficient for the thione is 8080 M^{-1} cm^{-1}. From the pyridine-2-thione concentrations, the quantity of SPDP on the surface was calculated giving the number of amino groups.

2.9. Reaction of Surface Amino Groups with Fluorescein Isothiocyanate. A 2.5 cm circular membrane of EVAL 27-T-NH_2, EVAL 44-T-NH_2, and PES-T-NH_2 was soaked in 15 mL of carbonate buffer, pH 9.5, to which an excess of (300 μL) fluorescein isothiocyanate (FITC, Aldrich) in DMSO (1 mg/mL) was added dropwise, at room temperature and left to react with the NH_2 groups for 2 h. The membranes were washed extensively with distilled water to remove all unreacted FITC from the membrane. The same procedure was done for silica-modified membranes without any coating present onto the surface as blank experiments. Using confocal microscopy on cross-sections of the membranes, the amino groups distribution can be deduced from the fluorescence image. The confocal microscopy used was a Zeiss LSM510.

2.10. Double-Stranded DNA Adsorption Isotherms. The membranes were cleaned by two different methods. One method employed 10% HCl solution as cleaning agent followed by thoroughly washing with distilled water and ethanol and drying. The other cleaning method employed an alkaline detergent, thoroughly washing with distilled water and ethanol, and drying and storing at 30 °C in a vacuum oven. A known weight of membranes (EVAL27, EVAL27-T, EVAL27-T-NH_2) was incubated for 24 h at constant temperature (37°C) with different concentrations of DNA (Calf Thymus DNA type I from Sigma) in 50 mM Tris/HCl pH 8 buffered 6 M perchlorate solutions.[13] The DNA concentration at equilibrium was determined using UV adsorption measurements performed at $\lambda = 259$ nm.

2.11. Membrane Characterization. Membrane morphology was imaged using a JEOL JSM-5600LV scanning electron microscope. The cross-section of the membranes was obtained by freeze fracturing the sample under liquid nitrogen. All the specimens were platinum coated with a JEOL JFC-1300 auto fine coater.

The pure water flux of unmodified and silica-modified membranes was determined using a dead-end ultrafiltration cell connected to a nitrogen gas cylinder to apply the feed pressure. The experiments were conducted at room temperature and different transmembrane pressures varying from 0.1 to 0.5 bar. The pure water flux was determined after steady-state conditions were reached. The same type of cell was used for liquid entry pressure measurements as characterization of hydrophobic-modified membranes. The liquid entry pressure was calculated using the Laplace-Young equation:

$$\Delta P = \frac{2\gamma_L \cos\theta}{r_{max}} \tag{1}$$

where γ_L is the surface tension of the liquid, θ the contact angle of the liquid with the surface, and r_{max} the maximum membrane pore radius as determined from a pore size distribution

Pore size distribution of the initial membrane was determined by the bubble point method using a Coulter Porometer II. The membrane was impregnated with Porofil (Aldrich). The needed pressure to expel the liquid from the pores was determined. The mean pore size is used to give an overall indication of the pore morphology; the largest pore size was used to estimate the liquid entry pressure.

Static water contact angles were measured using a goniometer (Dataphysics Contact Angle System). The sessile drop method was used to determine the static contact angle, θ, of the unmodified and modified membranes. The results are averages over at least 10 measurements on each sample.

The membrane porosity was determined from immersion experiments in water. The porosity results were correlated with porosity calculation from the absolute and apparent density measurements.

Membrane material density was measured by helium pycnometry, AccuPyc 1330 pycnometer. Twenty membranes with a diameter of 6 mm were used for the density measurements. To the same membranes, the apparent density was calculated making use of their weight, height, and diameter. Their difference quantifies the degree of macroporosity.

Swelling degree (SD) was determined by immersing a membrane for 24 h in a 50 mL vial containing distilled water. The swollen membrane was removed from the water and padded using a filter paper. The volume of wet and dry membranes were measured and used to calculate the swelling degree (in percent).

The surface modifications of the membranes were investigated with XPS (using Physical Electronics Quantera scanning X-ray microprobe) using a monochromatic Al Kα X-ray beam with a diameter of 100 μm was scanned over an area of 500 μm × 300 μm. In addition, the chemical structure of membrane surfaces were studied using ATR-FTIR (Bio-rad Digilab FTS60 FTIR spectrometer). The amount of silica on silica-modified membranes was determined by thermogravimetric analysis (TGA, Perkin-Elmer TGA 7, N_2 atmosphere and flow rates of 30 cm^3 /min).

Streaming potentials, ΔV, were measured as function of the nitrogen pressure drop, ΔP, across the membranes following the method.[29] Zeta potentials, ζ, were calculated from

$$\frac{\Delta V}{\Delta P} = \frac{\epsilon_0 \epsilon_r \zeta}{\eta \lambda} \tag{2}$$

where ϵ_0 is the vacuum permittivity, ϵ_r is the relative dielectric constant of the solution flowing through the membrane, and η is the solution viscosity. We used an aqueous 1 mM KCl solution prepared with MilliQ water at pH 5.5 with a measured electrical conductivity of $\lambda = 0.0185$ Ω^{-1} m^{-1}. For this solution, eq 2 leads to

$$\zeta = 0.262 \frac{\Delta V}{\Delta P} \tag{3}$$

with $\Delta V/\Delta P$ in mV/bar (see Figure 8).

3. Results and Discussions

3.1. Polymeric Membrane and Silica Hybrid. The Stöber synthesis comprises the hydrolysis and polymerization of TEOS to amorphous silica in an ethanol−ammonia mixture and has been applied to grow silica on a variety of inorganic colloids.[30,31] We have tested the suitability of the Stöber synthesis for silica deposition onto a polymeric membrane for three different types of macroporous membranes with different swelling degrees, hydrophilic properties, and morphologies. The preparation method for EVAL 44 and PES membranes is described in detail elsewhere.[26,32] However, for the EVAL 27 membranes, we first had to optimize preparation conditions (composition of the casting solution, coagulation bath temperature) as described in Section 2.3. We now briefly discuss some characteristics of the various membranes. SEM micrographs reveal an asymmetric membrane structures with a skin layer and a porous support having a pore size gradient (Figure 1) for all three membranes EVAL 27, EVAL 44, and PES. The morphological and permeation characteristics of the membranes are listed in Table 1.

(29) Nyström, M.; A Pihlajamäki, Ehsa, N. *J. Membrane Sci.*, **1994**, *87*, 245−256.

(30) Philipse, A. P.; Nechifor, A. M.; Patmamanoharan, C. *Langmuir* **1994**, *10*, 4451−4458.

(31) Philipse, A. P.; van Bruggen, M. P. B.; Patmamanoharan, C. *Langmuir* **1994**, *10*, 92−99.

(32) Boom, R. M.; Wienk, I. M.; Th. van den Boomgaard, Smolders, C. A. *J. Membr. Sci.* **1992**, *73* (2−3), 277−292.

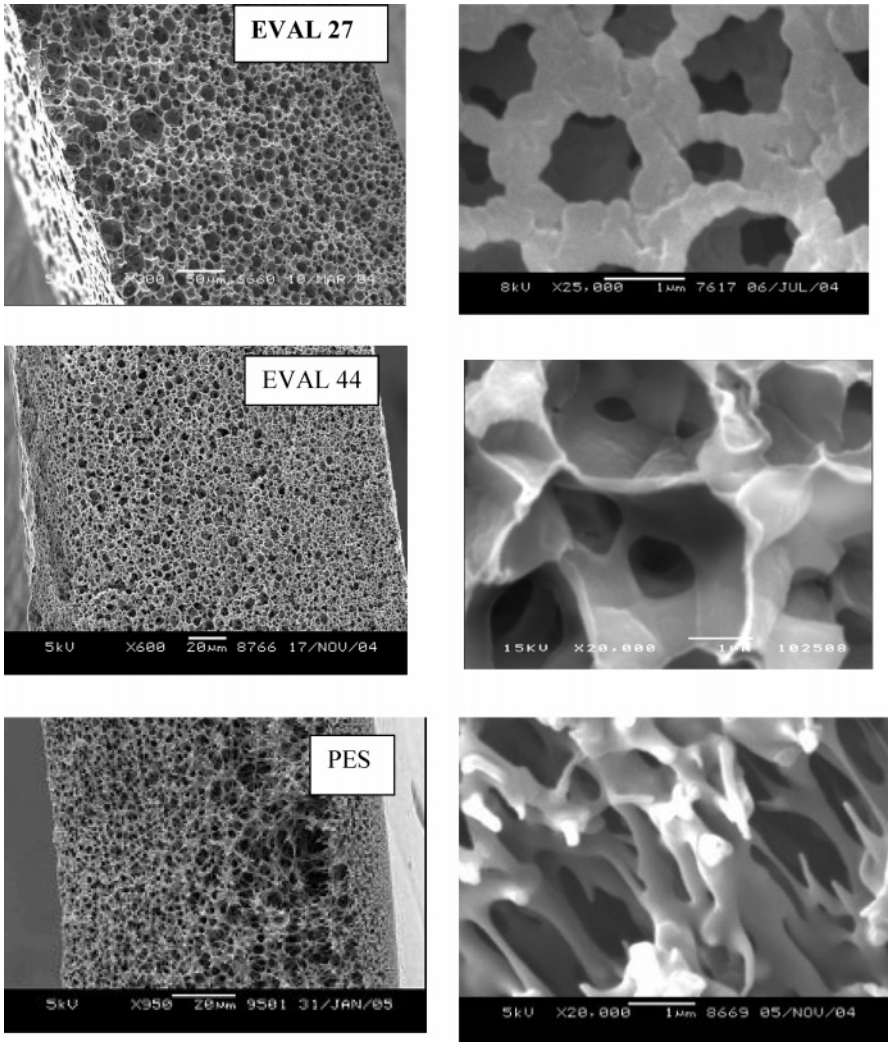

Figure 1. SEM micrographs of membrane cross sections (overview and detailed) before silica deposition.

Table 1. Membrane Properties of Precursor Membranes and Modified Membranes

	ρ_{abs} (g/cm^3)	ρ_{app} (g/cm^3)	porosity ϵ (%)	pore diameter[a] d_m (μm)	water permeance (L/m^{2}hbar)	TGA[b] (%)
			Unmodified Membrane			
EVAL 27	1.2	0.18	85 ± 2	0.5	8400	0.3
EVAL 44	1.2	0.23	80 ± 1	0.3	1700 ± 250	0.09
PES	1.67	0.21	83 ± 1	0.2	1700 ±250	32
			Silica-Modified Membrane			
EVAL 27 -T	1.34	0.2	85 ±1.5	0.45	10000 ±400	1.3
EVAL 44 -T	1.27	0.24	81 ±1	0.25	2000 ±200	4
PES -T	1.71	0. 28	80 ±1.7	0.143	2800	35
			Silica Growth Modified Membrane			
EVAL 27 -T−G	1.43	0.24	83	–	–	5
EVAL 44 -T−G	1.42	0.26	81	0.16	1800 ±300	6.9
PES -T−G	2.00	0.39		0.11	2500 ±150	42

[a] Median pore diameter. [b] The weight percent left after heating cycle is complete.

The prepared membranes proved to be stable in time. The silica layer is not affected by pure water flux measurements. Water fluxes slightly increased after silica deposition, despite the decrease of pore size. The observed increase in flux is most likely related to an increase in porosity due to the removal of polymeric species or the additive octanol during the membrane pretreatment with ethanol. Such removal could open part of the nonaccessible porosity in the membranes and, hence, the water flux increases. (Ethanol washing experiments on the polymeric precursor membranes also showed a flux increase.) This interpretation is consistent with the porosity measurements. When silica is deposited inside the membrane pore, we expect that the decrease in pore size (about 10%) would produce a decrease in the membrane porosity. However, the porosity of the membranes remains practically constant despite a smaller pore size.

In the Stöber synthesis,[18] silica spheres grow in a solution supersaturated with silicate species resulting from the hydrolysis and condensation of TEOS. It is difficult to discriminate between colloids growing in free solution or on the surface of the polymer precursor. During drying of the wet polymer samples, spheres

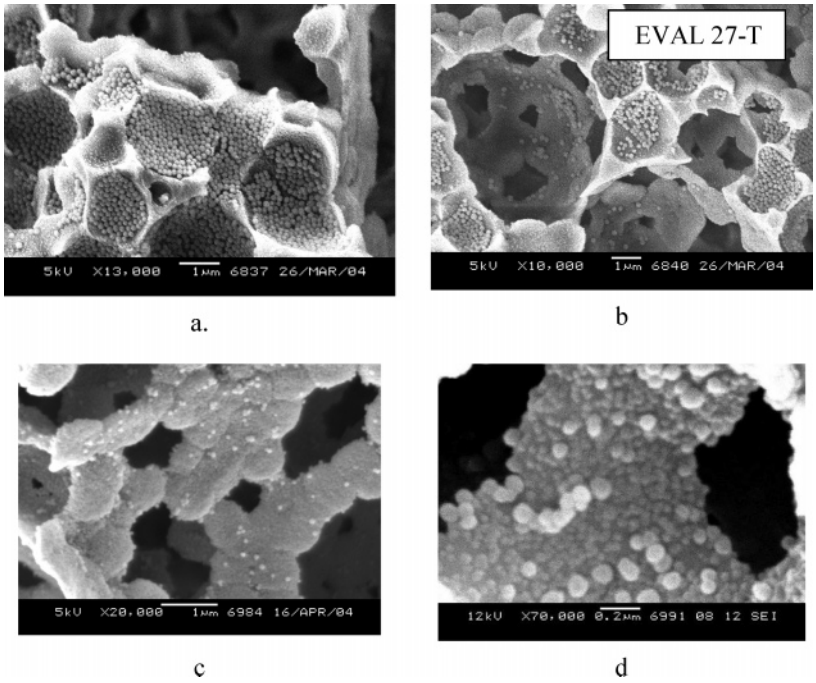

Figure 2. SEM images of silica-modified EVAL 27 macroporous material. The morphology shows evidence of deposition of preformed silica spheres (top), as well as heterogeneous silica nucleation directly on the polymer surface (below).

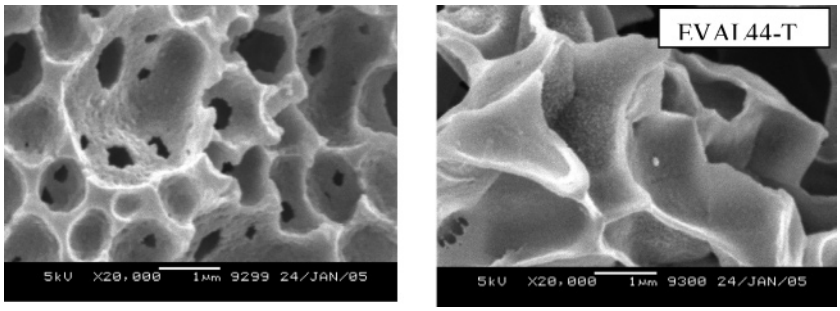

Figure 3. Illustrative examples of silica deposition on EVAL 44 membranes in a form of a fairly uniform silica layer.

formed in free solution may adsorb onto a polymeric substrate, resulting in a neatly ordered arrangements of large silica spheres, as observed in the SEM pictures of membranes in Figure 2a and b. However, there exists in most cases a continuous layer of much smaller silica particle, as visible in Figure 2c and d. The small spheres appear to be fused into a continuos layer covering all of the polymer struts. We hypothesize that silica must directly nucleate and grow on the membrane surface with the surface acting as a catalyst that lowers the activation energy for particle formation.[33] (Note also that the membranes in the Stöber solution have been previously swollen in ethanol−ammonia, which can also promote silica nucleation on the membrane surface.) For this heterogeneous nucleation, only a modest affinity between a surface and the newly formed phase is needed; a high supersaturation can only be maintained near a surface when the surface is nearly completely nonwetting for the new phase.[33] Figure 2c suggests that silica particles indeed have been formed directly on the membrane surface: their morphology clearly differs from the smooth silica spheres usually resulting from homogeneous nucleation. The hydroxyl groups on the surface of the macroporous EVAL certainly contribute to the affinity for TEOS or silicate species derived from it. PES presumably has less interaction with TEOS derivates, but apparently the 'wetting' of the polymer by silica is still sufficient to induce heterogeneous silica growth, as shown in Figure 4. In some particular cases, one can observe the presence of a distinct continuous silica crust around a polymeric strut, as shown in Figure 4a and Figure 6e.

The presence of silica on the membrane surface is further confirmed by XPS and IR analysis (see Tables 2 and 3 for detailed XPS results and Figure 5 for IR spectra). The XPS data support the presence of the Si as new element next to already present carbon and oxygen in the polymeric precursors. For example, the initial EVAL 27 membrane contains no detectable silicium, whereas the silica-modified membrane yields an atomic concentration of about 24% for silicium on the surface (see Table 3).

The difference between the IR spectra of the precursor membranes of EVAL 27 and EVAL 44 (Figure 5a) is minimal. Both materials contain the same backbone and functional groups, the difference being only the ratio between the hydrophilic and hydrophobic part of the copolymer. In contrast, the spectra of the EVAL membranes and PES are very different (see Figure 5a and b). However, after silica deposition, the spectra are very similar (Figure 5c). The silica material clearly shows a strong band near 1070−1100 cm^{-1} attributed to Si−O−Si asymmetric stretching. Unmodified EVAL 27 shows a clearly broad bond 3200−3400 cm^{-1} that corresponds to O−H stretching vibrations of the hydroxyl groups. The intensity of this band is decreasing significantly due to the presence of silica material on the

(33) Philipse, A. P. Particulate colloids: Aspects of preparation and characterization. In *Fundamentals of Interfaces and Colloids Science*; Lyklema, J., Ed.; Elsevier: New York, 2005; Vol. IV.

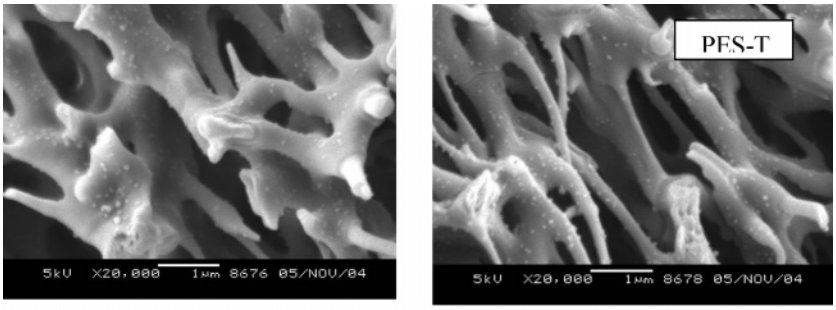

Figure 4. Example of SEM pictures of silica-modified PES membranes. The images show the presence of a fairly uniform silica layer and dispersed larger silica particles attached to it.

Table 2. XPS Results for EVAL 27

	C [%]	O [%]	Si [%]	N [%]	F [%]	O/C [%]	N/C [%]	Si/C [%]	F/C [%]
EVAL27	72.5 ± 0.6	27.5 ± 0.6	–	–	–	0.38	–	–	–
EVAL27-T	14. 6 ± 0.8	61.3 ± 0.7	24.2 ± 0.3	–	–	4.2	–	1.67	–
EVAL27 T-FOTS	23.1 ± 0.3	34.5 ± 0.2	14.2 ± 0.5	–	28.3 ± 0.4	1.5	–	0.61	1.23
EVAL27-T-NH_2 prepared in toluene or THF	30.4 ± 2	49.2 ±1.6	18.3 ±0.8	2.1 ±0.2	–	1.61	0.06	0.6	–
EVAL27-T-NH_{2-} prepared in ethanol	36.9 ±0.3	43.4 ±0.3	17 ±0.1	3.3 ±0.02		1.18	0.09	1.18	–

Table 3. XPS of PES

	C [%]	O [%]	S [%]	Si [%]	N %]	F [%]	O/C [%]	N/C [%]	Si/C [%]	F/C [%]	S/C [%]
PES	73 ±0.9	18.2 ± 0.9	2.98 ±0.1	0.5 ±0.2	5.3 ±0.2	–	0.25	0.07	0.006	–	0.04
PES-T	22.1 ±0.5	55.4 ±0.5	–	20.8 ±0.2	–	–	2.5	-	0.94	–	–
PES T-FOTS	23.6 ±0.5	23.2 ±0.5	–	9.9 ±0.2		43.4 ±0.5	0.98	-	0.42	1.85	–
PES-T-NH2	20 ±0.8	55 ± 0.5	0.33	22.4 ±0.2	2.1 ±0.2	–	2.75	0.1	1.12	–	0.02

membrane. Further, EVAL 27 membranes show multiple bands around 1100 cm^{-1} that are assigned to C−O stretching and 1100−1200 cm^{-1} assigned to secondary alcohol stretching. Also, comparing the PES spectra and the silica modified PES membranes, we clearly observe the disappearance of the adsorption bonds S═O (1150, 1323 cm^{-1}) and the aromatic C═C stretching vibration (1485, 1578 cm^{-1}).

TGA and mass density measurements indicate that the silica weight fraction of the hybrid membranes is about 3−5% (see Table 1). Figures 4a and 6e suggest the layers to be around 50−100 nm thick.

The silica layer influences the surface properties of the membrane, as judged from the contact angles (Table 4). For all three membranes (EVAL 27, EVAL 44, and PES), the contact angle exceeds 90° once an initial silica layer is present as synthesized in the first step. The origin of this increase in contact angle, θ, is difficult to explain and may be related to ethoxy groups that are known to be present on Stöber silica,[8] as well as the complex wetting behavior of macroporous materials. The presence of ethoxy groups on the silica surface during the first deposition cycle is supported by the carbon content measured with XPS (Tables 2 and 3). A detailed mechanism explaining the initial rise of the contact angle is beyond the scope of the contribution. More important is the preparation of a very hydrophilic native silica layer.

To obtain a native silica surface, we performed a subsequent repetition of the deposition procedure (abbreviation *x*-T−G). SEM images clearly reveal that the small silica cluster from the first deposition grow to larger particles that are embedded in the silica layer for EVAL 27 silica modified membranes (see Figure 6). Also, density and TGA measurements showed an increase of silica concentration by 2−3% in weight for the first layer deposition to approximately 6% after the silica grow experiment. For PES membranes, we encounter another behavior during further silica growth and observe a bridging between existing small silica particles, leading to a more uniform silica layer as compared to silica-modified EVAL 27 membranes. Also, density and TGA measurements show an increase in the silica content from 3% for PES-T to over 7% for PES-T−G.

Increase of silica content inside the membranes modifies not only the membrane density but also the hydrophilicity and dynamic flow behavior. The membranes become extremely hydrophilic and the contact angle becomes nearly zero for all three modified membranes (see Table 4). Liquid entry pressures cannot be determined because the membranes wet immediately upon contacting with water. Increase in silica content can alter the mechanical properties of the membranes. For almost all membranes presented here, flexibility remains good. However, further growth of the silica crust can result in brittleness of the membranes.

3.2. Silylated Silica Membranes. The silica layer on the membrane surface contains silanol groups that react easily with silylating agents in the form of a silane-coupling agents (SCA). The latter contain silicon−alkoxide or silicon−chloride groups that hydrolyze and condense with surface silanol groups such that functional groups from the SCA are covalently linked to the silica. The SCAs used in this study have three hydrolyzable groups which promotes the formation of multilayers on silica, as has been observed for the case of colloidal sols.[8] We will now discuss several experimental results that demonstrate the presence of a nondesorbing silane multilayer on our polymer-in-a-silica-crust membranes and their properties being almost independent of the precursor material.

The presence of the hydrophobic silane-coupling agent (FOTS and OTS) is demonstrated directly by XPS analysis (see Tables 2 and 3) and indirectly by contact angle measurements (see Table 4). Fluor could be determined only on surface-modified silica

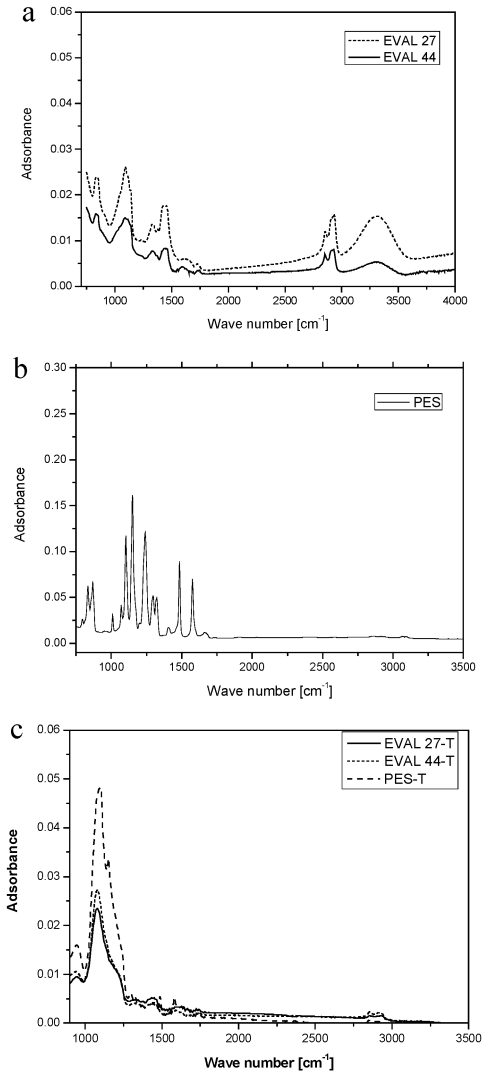

Figure 5. IR spectra of the unmodified and silica-modified membranes, (a) EVAL 27 and EVAL 44; (b) PES; (c) EVAL27-T, EVAL 44-T, PES-T. The spectra shows clearly the that all three silica-modified membranes show an almost identical spectrum, independent of the initial membrane material.

membranes (EVAL27-T-FOTS and PES-T-FOTS) but did not appear in any other membrane.

The contact angle of all three membranes strongly increases from nearly zero for the silica-modified membranes to around 129−145°, exceeding the value of $\theta = 115°$ found for hydrophobic smooth FOTS surfaces.[34] The difference is very likely due to surface roughness of the silica membranes that enlarges the contact angle for a hydrophobic material (often referred to as the Lotus effect[35]). Indeed, for EVAL 44-T-FOTS, the contact angle is about 120°, much lower than for EVAL 27-T-FOTS or PES-T-FOTS (see Table 2). Comparing the silica layers of the three membranes, we can clearly see that for EVAL 44-T the layer is smoother then for the other two membranes.

Hydrophobic porous membranes do not permit water flow below a certain liquid entry pressure (LEP). This critical pressure difference is correlated to the interfacial tension (for water, 72 mN/m), the contact angle of the liquid on the surface, and the size and shape of membrane pores (eq 1).[36] However, polymeric membranes possess interconnected pores with irregular pore shapes and different roughness of the internal and external surface. In addition, polymeric membranes have a pore size distribution of the pores, so when pressure is applied, water will penetrate first the largest pore, which actually determines the value of LEP. For the calculation of the LEP, we used as radius the maximum value obtained from coulter porometry measurements. For instance, we estimate the LEP for EVAL 27-T-FOTS ($r_{max} = 1.08$ μm being different from the median pore diameter as listed in Table 1) to be around 2.06 bar, which is close to the experimental value of 1.9 bar. Table 5 shows that estimated and measured LEP agree well.

We can conclude that, independent of the chemical nature of the polymeric precursor material, all silica hybrid membranes have quite similar characteristics. Being subsequently subjected to a silane coupling agent, specific surface functionality can be designed. Another example of this surface tailoring is demonstreated by the amination of the silica-modified membranes using APS. APS is extensively used for silica gel modification for biomolecule immobilization.[7] APS reaction with silica surfaces is usually done in dry organic solvents such as THF and toluene.[37] The same procedure was followed for EVAL membranes. We could not use the same conditions for PES-T membranes, so an alternative method of APS silylation of macroporous polymeric materials was applied, as described in Section 2.7.4. XPS data in Tables 4 and 5 support that both methods showed that the silane-coupling agent APS reacts with the silica surface independent of the starting polymeric membrane. The amino group distribution was visualized after FITC labeling by confocal fluorescence microscopy, as shown in Figure 7, indicating that amino groups are uniformly distributed inside the silica-modified membranes. In addition, the average intensity reveals that the highest concentration of amino groups is found on EVAL44-T-NH_2 membrane (intensity average about 250) followed by EVAL 27- T-NH_2. The lowest amino concentration (intensity average is about 120) is found for the PES-modified membranes, while for silica-modified membranes, no fluorescence was found. These results are also confirmed by SPDP quantitative determination of amino groups (surface concentration of amino 2.8×10^{-10} mol/cm^2 for EVAL 27-T-NH_2, considering the membrane surface as measured by BET 7.8 m^2/g, 11×10^{-10} mol/cm^2 for EVAL 44-T-NH_2, for BET surface area 10 m^2/g, and 10^{-10} mol/cm^2 for PES-T-NH_2 for 4.7 m^2/g).

The zeta potentials listed in Table 6 are obtained from the streaming potentials experiments visualized in Figure 8 using eq 2. It should be noted that eq 2 is valid for any pore geometry as long as the pore radius of curvature is large relative to the Debye length, κ^{-1}, of the solution.[38] For 1 mM KCl, $\kappa^{-1} = 9.8$ nm, so this condition is satisfied in view of the pore sizes (see pore diameters listed in Table 1). In addition, eq 3 assumes absence of surface conductivity, a conductivity that could play a role when bulk conductivities are low. Surface conductivity reduces ΔV and lowers the apparent value of the zeta potential.[38] Surface roughness (due to silica particles, for example) also lowers the measured ζ since it increases the stagnant solvent layer thickness on a surface such that the slipping plane is further away from the membrane surface. Thus, the ζ values in Table 6 very likely represent a lower bound on the zeta potential. Even with this reservation, the zeta potential values clearly manifest the various surface treatments of the membranes. For example,

(34) Geerken, M. J.; van Zanten, T. S.; Lammertink, R. G. H.; Borneman, Z.; Nijdam, W.; van Rijn, C. J. M.; Wessling, M. *Adv. Eng. Mater.* **2004**, *6* (9), 749−754.

(35) Neinhuis, C.; Barthlott, W. *Ann. Bot.-London* **1997**, *79*, 667−677.

(36) Garciya-Payo, M. C.; Izquierdo-Gil, M. A.; Fernandez-Pineda, C. *J. Colloid Interface Sci.* **2000**, *230*, 420−431.

(37) Etienne, M.; Walcarius, A. *Talanta* **2003**, *59* (6), 1173−1188.

(38) Overbeek, J. Th. In *Colloid Science Interface*; Kruyt, H. R., Ed; Elsevier: Amsterdam, 1952.

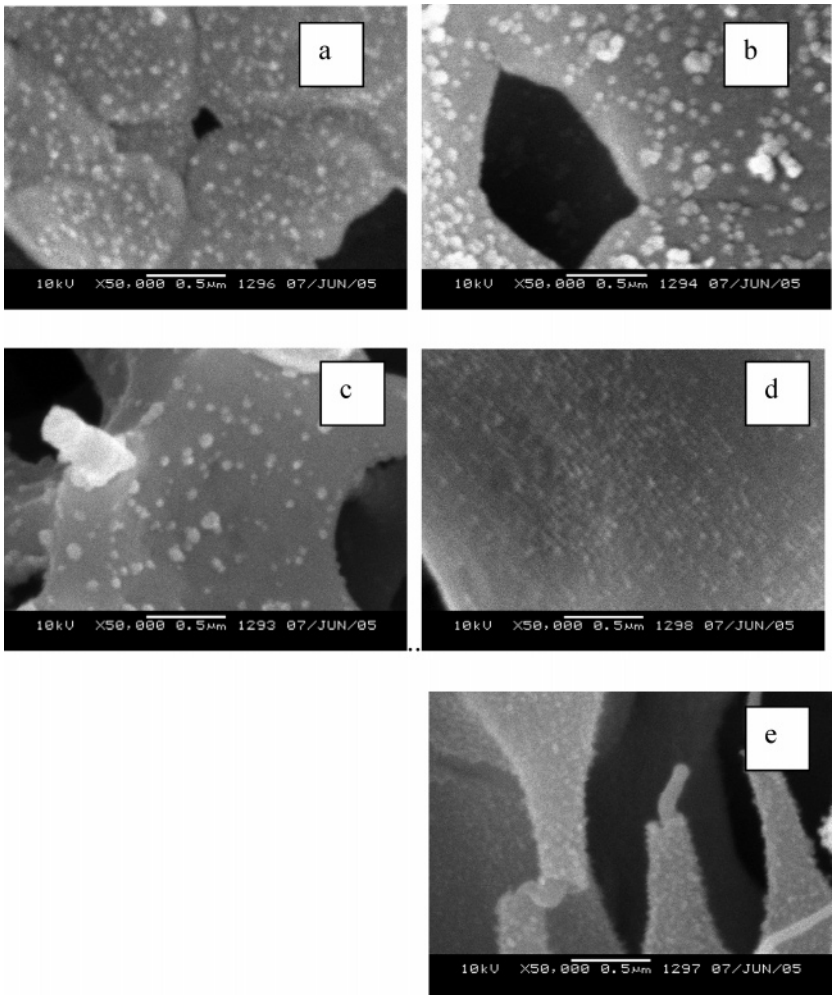

Figure 6. Examples of SEM micrographs of silica-modified membranes [(a) EVAL 27-T; (c) PES-T] and silica growth [(b) EVAL 27-T−G, (d) and (e) PES-T−G] on the silica-modified membranes.

Table 4. Contact Angle of Unmodified and Modified Membranes

	unmodified membrane	silica membrane	silica growth[a]	FOTS silica membrane	OTS silica membrane
EVAL27	70.1 (±1.2)	93.7	0	145.5 (±1.8)	127.7 (±2.1)
EVAL44	89.9 (±2.6)	92.6 (±2.8)	0	125.5 (±1.8)	(n.a.)
PES	62 (±1.9)	91 (±2.5)	0	142.1 (±1.5)	(n.a.)

[a] Very hydrophilic, too low to measure accurately.

Table 5. Experimental and Calculated Liquid Entry Pressure (LEP) for Surface Functionalized Polymer-in-a-Silica-Crust Membranes

LEP[bar]	EVAL27-T-OTS	EVAL27-T-FOTS	EVAL44-T-FOTS	PES-T-FOTS
calculated	1.3	2.1	2	3.7
experimental	1.0	1.9	−[a]	3

[a]Too brittle to resist the pressure.

for PES membranes we find $\zeta = -1.7$ mV (in good agreement with results in ref 39), whereas for PES-T−G, the zeta potential has dropped to −4.9 mV, consistent with the presence of silica species on its surface. When the silica on PES-T−G is subsequently modified with amino groups, the zeta potential switches the sign and ζ becomes 4.95 mV (Table 6). The substantial increase in ζ due to amino groups is observed for all membranes. However, cleaning of the amino-modified membranes renders them negative again. The effect of cleaning the membranes with various solutions is discussed in detail below.

3.3. DNA Adsorption Experiments. DNA adsorbs onto silica and aminated silica surfaces, as described in refs 13, 25. The adsorption of DNA on silica has the purpose for removing the DNA only: one is generally not interested in the desorption or recovery of DNA. (Conformation changes of DNA due to adsorption and desorption is of less practical relevance.) Adsorption experiments with the polymeric precursor and silica-modified membranes reveal that the presence of silanol groups strongly increases the amount of DNA adsorption (Figure 9). The presence of NH_2 groups further enhances the DNA adsorption capacity of the polymers in a silica crust. Adsorption is related to entropy, with little or no enthalpic effects being present.[13] At such high ionic strength of the solution, three effects cause entropically driven adsorption: (a) shielded intermolecular electrostatic forces, (b) dehydration of the DNA and silica surfaces, and (c) some intermolecular hydrogen bond formation

(39) Pontie, M.; Chasseray, X.; Lemordant, D.; Laine, J. M. *J. Membr. Sci.* **1997**, *129*, 125−133.

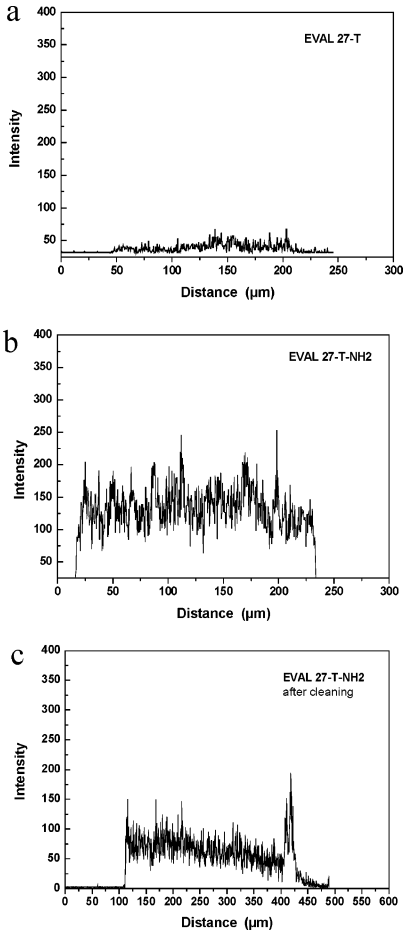

Figure 7. Example of confocal microscopy intensity profile for (a) a silica-modified membrane EVAL27-T, (b) an aminated surface EVAL-27-T-NH_2, and (c) an aminated membrane that was subjected to a thoroughly cleaning procedure for DNA adsorption experiments. The graphs clearly show the presence of amino groups onto the surface compared with the bare silica surface and a loss of amino groups during the cleaning procedure.

Table 6. Streaming Potential Values for Unmodified, Silica-Polymeric Hybrid, and Aminated Membranes

membrane	*z* [mV]
Unmodified Membrane	
EVAL 27	−14.8
EVAL 44	−19.1
PES	−1.7
Silica Growth Modified Membrane	
EVAL 27 -T−G	−12.05
EVAL 44 -T−G	−13.4
PES -T−G	−4.9
Aminated Surface-Modified Silica Membranes	
EVAL 27 -T-NH_2[a]	5.48
EVAL 44 -T-NH_2	4.74
PES -T-NH_2	4.95

[a] Streaming potential becomes −7.1 (mV) after cleaning procedure EVAL 44.

in the DNA−silica contact layer. Hence, the interaction between the DNA molecules and (silylated) silica is independent of the surface charge. The high ionic strength of perchlorate solution screens the negative or positive charge of the bare and aminated silica, as well as the charges present on the double-stranded DNA molecule. The presence of high salt concentration, however, can dehydrate DNA molecules, driving the DNA polymer to attach to the silica surface. The adsorptions capacity, nevertheless, is still significantly lower than the data on silica particles reported

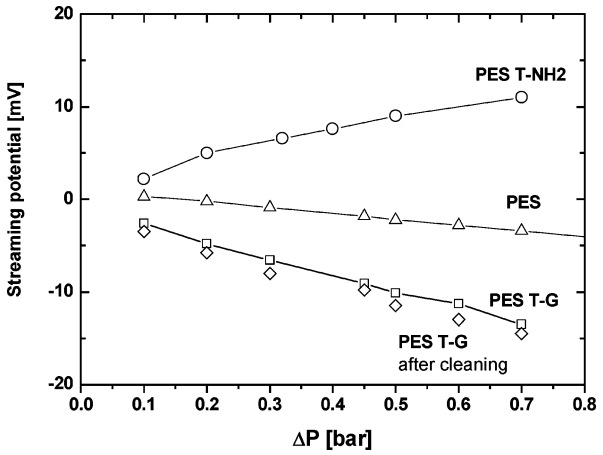

Figure 8. Streaming potential measurements results for aminated, polymer-in-silica-crust macroporous material, and unmodified polymer macroporous material.

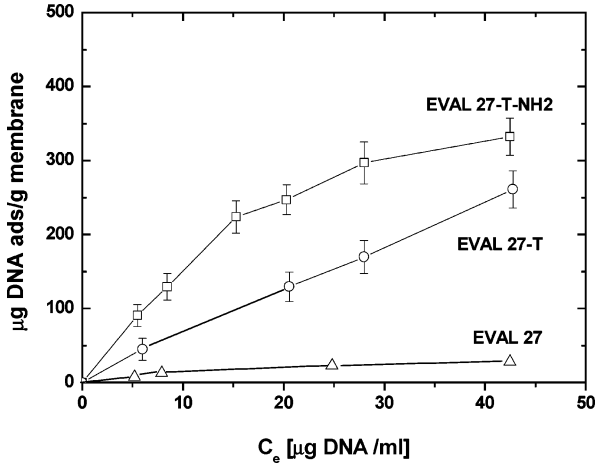

Figure 9. DNA adsorption isotherm. The graph shows that silica surface and the aminated surface are suitable for DNA adsorption.

in ref 13. A possible explanation is related to the surface availability.

In the literature, working protocols were developed for DNA adsorption onto silica particles in which first silica particles were thoroughly cleaned with aggressive agents.[13] However, silica-crust hybrid membranes cannot be treated in harsh conditions. The silica crust on the membranes is not a continuous film but, as described earlier, is formed by deposition of discrete silica particles onto the membrane surface. We observed that the membrane pretreatment could decrease or increase the DNA adsorption. Treating the membranes with 10% hydrochloric acid followed by flushing with water and ethanol in fact destroys any adsorption functionality of the silica surface, leading to a DNA adsorption close to zero for all the modified membranes. The polymeric membrane support can withstand neither treatment at elevated temperature with $K_2Cr_2O_7$ acid solutions nor with 32% hydrochloric acid.[13] On the other hand, the polymer−silica hybrid membrane one may consider to reactivate the surface silanol groups with an alkaline detergent which removes organic material that may be attached to the membrane surface. The main drawback of using alkaline detergent is a slight dissolving of silica from the surface and partial hydrolysis of the SCAs depending on time and pH. Streaming potential measurements also manifested the changes in surface charge due to an alkaline cleaning procedure. The surface charge of SCA-modified silica membranes changes slightly when treated with alkaline detergent, as we can observe from Figure 8. In the case of the aminated surface,

treatment with an alkaline detergent dramatically changes the surface properties, as we can conclude from streaming potential measurements (see Table 6). As an example, we can compare the values obtained for EVAL 27-T-NH_2 before (+5.48 mV) and after the cleaning procedure (−7.1 mV) but still less than the streaming potential of silica modified membranes (−12.1 mV). However, confocal microscopy gives evidence that amino groups are still present on the surface (Figure 7c). We interpret this in terms of strong adsorption of surface active ingredients (i.e., surfactants) to the positive aminated silica surface: this does not reduce the fluorescence signal in the confocal microscopic analysis but dominates the charges in the streaming potential experiment.

4. Conclusions

We have shown that alkaline hydrolysis of tetraethoxysilane inside various polymer matrices leads to coverage of the polymer surface with an amorphous silica crust. The silica allows subsequent functionalization with hydrophobic, as well as hydrophilic silane coupling agents. The properties of the functionalized macroporous structure are independent of the type of the starting polymeric substrate that merely provides the architecture of the pore structure without affecting the substrate chemistry and affinities of the silica crust. The potential of our polymer in a silica crust material is illustrated by the more then 10-fold increase in adsorption capacity for double-stranded DNA in comparison to that of a bare polymer matrix.

Acknowledgment. This work was financially supported by the Dutch Economy Ecology Technology (EET) program. Dr. Ing. Ine Segers-Nolten from the Biophysical Engineering Group University of Twente is thanked for kindly providing the DNA, Dr. Arto Philajamaki from Lappeenranta University of Technology, Finland for providing us with the streaming potential cell, and Zandrie Borneman, Wilbert van de Ven, and Maik Geerken for their support of this research.

LA060137O